# Global Investigation on the Potential Energy Surface of $CH_3CN$: Application of the Scaled Hypersphere Search Method

**Xia Yang, Satoshi Maeda, and Koichi Ohno***

*Department of Chemistry, Graduate School of Science, Tohoku University, Aramaki, Aoba-ku, Sendai 980-8578, Japan*

*Received: April 21, 2005; In Final Form: June 24, 2005*

An extensive quantum chemical study of the potential energy surface (PES) for all possible isomerization and dissociation reactions of $CH_3CN$ is reported at the DFT (B3LYP/6-311++G(d,p)) and CCSD(T)/cc-pVTZ//B3LYP/6-311++G(d,p) levels of theory. The pathways around the equilibrium structures can be discovered by the scaled hypersphere search (SHS) method, which enables us to make a global analysis of the potential energy surface for a given chemical composition in combination with a downhill-walk algorithm. Seventeen equilibrium structures and 59 interconversion transition states have been found on the singlet PES. The four lowest lying isomers with thermodynamic stability are also kinetically stable with the lowest conversion barriers of 49.69−101.53 kcal/mol at the CCSD(T)/cc-pVTZ//B3LYP/6-311++G(d,p) level, whereas three-membered-ring isomers c-$CH_2NCH$, c-$CH_2CNH$, and c-CHNHCH can be considered as metastable intermediates which can further convert into the low-lying chainlike isomers and higher lying acyclic isomers with the lowest conversion energies of 21.70−59.99 kcal/mol. Thirteen available dissociation channels depending on the different initial isomers have been identified. A prediction can be made for the possible mechanism explaining the migration of a hydrogen atom in competition with the CC bond dissociation. Several new energetically accessible pathways are found to be responsible for the migration of the hydrogen atom. The present results demonstrate that the SHS method is an efficient and powerful technique for global mapping of reaction pathways on PESs.

## 1. Introduction

Acetonitrile ($CH_3CN$) is an important intermediate in a number of combustion processes,[1] including biomass burning, internal combustion engine burning, and so on. $CH_3CN$ then diffuses into the stratosphere, in which it is progressively destroyed through chemical reactions.[2] Reactions of $CH_3CN$ are also of interest in atmospheric chemistry,[3] since acetonitrile is a ubiquitous trace gas in the atmosphere—one of the largest global pollution sources.

It is well-known that the temperature and pressure strongly affect the reaction of organic compounds in terms of the reaction pathway and products, reaction rate, and activation energy. The capability of supercritical conditions to produce desired compounds in the degradation pathway of organic molecules, such as the use of high-temperature and high-pressure water, has recently attracted attention for the destruction of various organic substances, the oxidation of biomass and metabolic wastes, and the development of new chemical synthesis strategies for waste recycling.[4−7] This makes it possible to design an industrial process to decompose or transit acetonitrile into combustible gas mixtures or an alternative in which new carbon−carbon, carbon−oxygen, and carbon−hydrogen bonds can be produced. Although photodissociation of $CH_3CN$ and $CH_3NC$ and the reactions of $CH_3CN$ with the highly reactive radical species such as F, Cl, O($^3$P), and OH have been fairly well investigated experimentally,[8−11] available theoretical data are not sufficient to elucidate the mechanism of the reaction, which may produce $CH_3CN$ or convert $CH_3CN$ into other species. Several previous theoretical studies have focused on direct dynamical properties for the reactions X + $CH_3CN$ (X = Cl, Br, H).[12,13] However, the detailed dissociation information on this system is lacking. Some dissociation products, such as $C_2H_2$ + NH, $CH_3$ + CN, NCCH + $H_2$, and $C_2NH$ + $H_2$, which are also important intermediates in many high-temperature and -pressure processes such as the formation of polyaromatic hydrocarbons and soot in hydrocarbon combustion and chemical vapor deposition of diamond,[14−16] should also be considered from a theoretical viewpoint.

Thereby, future experimental reinvestigation on the product distributions of $CH_3CN$ at high temperature and pressure are expected to greatly help in the chemical modeling of those complex systems, where few direct data are available. A recent experiment has shown that the hydrogen atom migration proceeds in competition with the two-body Coulomb explosion of acetonitrile.[17] The unimolecular dissociation of the acetonitrile molecular cation ($CH_3CN^{\bullet+}$) has been investigated using mass-analyzed ion kinetic energy spectrometry.[18] Some stable isomers of $C_2H_3N^{\bullet+}$ have been suggested in the CID studies by two research groups.[19,20] On the basis of the experimental findings alone, it has been very difficult to draw definite conclusions concerning the role of isomerization in the molecular dissociation process. Only the results of quantum chemical calculations were reported for some $C_2H_3N^{\bullet+}$ [21] and $C_2H_2N^{\bullet+}$ [22−24] isomers. It is worthwhile to investigate theoretically the pathways of isomerization and dissociation of the neutral molecule $CH_3CN$, which have not been understood clearly in the previous experimental studies. Thus, to fully address the kinetics of this unimolecular reaction and mechanism of isomerization theoreti-

* To whom correspondence should be addressed. E-mail: ohnok@qpcrkk.chem.tohoku.ac.jp.

10.1021/jp052067k CCC: $30.25 
Published on Web 07/23/2005

cally, a potential surface that is fully global needs to be investigated.

However, it has been very difficult to obtain a global survey of a multidimensional potential energy surface (PES) because of more troublesome uphill walking in comparison with downhill walking and huge computational demands. Recently, the scaled hypersphere search (SHS) method has made it possible to survey global reaction pathways on a PES starting from a known structure.[25,26] The SHS method made use of scaled normal coordinates to transform a reference hypersurface into a hypersphere surface on which every point should have the same energy when the potentials are harmonic. This treatment is very important, since reaction paths are not always along particular normal coordinates but possibly along oblique directions corresponding to mixtures of several coordinates. The SHS method can be used to locate all reaction paths leading to anharmonic downward distortions of the PES. Its application to a one-point method has succeeded in discovering new reaction pathways yielding a glycine molecule ($H_2NCH_2COOH$) from $CH_2$, $NH_3$, and $CO_2$.[27,28] In addition, this approach is found to lead to an efficient and accurate estimate of a transition state (TS) region without any initial guesses using a two-point method for an isomerization reaction of HCN, $(H_2O)_2$, and alanine dipeptide.[29]

In this study, a global potential energy surface that contains an isomerization mechanism of $CH_3CN$ as well as molecular and radical dissociation channels is obtained by employing the SHS method, which is helpful to understand and disclose the likely reaction mechanism more clearly and interpret the available experimental results more reasonably. In addition to the experimentally known isomers, various new isomers are found to possess high or moderate kinetic stabilities toward isomerization or dissociation.

## 2. Computational Methods

Reaction pathways around the equilibrium structures of acetonitrile were first searched on the singlet PES at the HF/6-31G level of calculations by the SHS method,[25,26] in which harmonic vibrational frequencies at the same level and intrinsic reaction coordinate (IRC) calculations[30−33] were carried out, to check whether the obtained structure is a minimum or a saddle point and to test whether the transition state connects the right isomers or not, respectively. There are 21 equilibrium structures (EQs) and 86 interconversion TSs found from the SHS method.

Next, structures of all the singlet minima obtained as well as those of the singlet transition states involved in the SHS method were further refined at the DFT/B3LYP/6-311++G(d,p) level of calculation. A total of 17 minimum isomers and 59 transition states are ultimately located at the B3LYP/6-311++G(d,p) level by geometry optimizations using structures obtained by the low-level calculation as initial guesses. IRC calculations starting from each TS on the B3LYP/6-311++G(d,p) surface were also made to confirm the connection between each EQ. Four minima corresponding to $CH_2CHN$ and $CHCH_2N$ chain structures of very shallow wells on the HF/6-31G surface vanished. In connection with them, transition structures for reactions of their isomerizations and dissociations were also lost. Some other transition structures placed in the higher energy area of the HF/6-31G surface also vanished according to the difference between Hartree−Fock and density functional calculations. To gain reliable relative energies of each stationary point on the PES, single-point calculations with the ab initio coupled-cluster singles and doubles method including a perturbative estimate of triples (CCSD(T))[34] were performed employing the correlation-consistent polarized valence triple-$\zeta$ (cc-pVTZ) basis set.[35−37] The CCSD(T)/cc-pVTZ//DFT/B3LYP/6-311++G(d,p) relative energies discussed below and shown in the figures of the pathways include the zero-point vibrational energy (ZPE) corrections estimated by the DFT/B3LYP/6-311++G(d,p) level of calculations with a scaling factor of 0.96. All calculations (except for the SHS procedures) were carried out using the Gaussian03 program package.[38]

## 3. Results and Discussion

Although some reactions of acetonitrile with molecules or radicals and some other analogous [$C_x$, $H_y$, N] ($x = 2, 3$; $y = 3, 4, 5$) species have been studied previously at different computational levels,[12,13,39−43] no systematic theoretical study of the $CH_3CN$ isomers has been reported. The present calculations have revealed 17 equilibrium structures labeled as EQ*n* (*n* from 0 to 16) and 59 transition states marked as TS*n*/*m* (or TS*n*/*m*(*i*)) for connecting directly with EQ*n* and EQ*m* or TS*n*/D (or TS*n*/D(*i*)) for a dissociation pathway starting from EQ*n*, as shown in Figures 1−3, respectively. The character *i* in parentheses denotes the *i*th transition state in the reaction EQ*n* → EQ*m* or the *i*th dissociation channel for EQ*n*. The corresponding symmetries and relative energies of all the species calculated at the DFT/B3LYP/6-311++G(d,p) and CCSD(T)/cc-pVTZ//B3LYP/6-311++G(d,p) levels are summarized in Table 1. The possible dissociation channels and relative energies of the dissociation products are listed in Table 2, and the corresponding structures are also shown in Figure 4. Finally, schematic energetic profiles of the singlet PES for [$C_2$, $H_3$, N] isomerization and dissociation channels are plotted in Figures 5 and 6, respectively, in which possible connections between various forms of isomers are illustrated at the ab initio CCSD(T)/cc-pVTZ//DFT/B3LYP/6-311++G(d,p) level.

**3.1. EQs of the [$C_2$, $H_3$, N] System.** On the singlet [$C_2$, $H_3$, N] PES, 14 acyclic isomers and 3 monocyclic structures were characterized as minima. The two lowest lying isomers are acetonitrile EQ0 (0.00 kcal/mol) and methyl isocyanide EQ1 (24.10 kcal/mol), each of which possesses $C_{3v}$ symmetry. Structurally they can be viewed as the combination between $CH_3$ and C≡N radicals. The C atom has much higher spin density (0.841e) than the N atom (0.159e) in the CN radical; thus, the $CH_3$ attack at the C site should be more favored than at the N site.

Nearly all chainlike isomers and cyclic isomers (EQ0−EQ7 in Figure 1) have high thermodynamic stability (according to the relative energy order) as compared to the remaining acyclic structures, which lie within a range of relative energies from 0.00 to 81.83 kcal/mol, while other acyclic isomers are from 90.23 to 132.40 kcal/mol with respect to the global minima. Clearly, this may not be the reason that the acyclic isomers are devoid of strain due to smaller ring or structural constraints existing in cyclic isomers. Hence, the relative energies of these isomers may be decided mainly by the subtle electronic factors due to the number and positioning of sp, $sp^2$, and $sp^3$ carbons and various types of bonds. The isomers having relatively high thermodynamic stability are the ones possessing fewer lone pairs of electrons in the molecule; e.g., more energetically stable chainlike isomers and cyclic isomers (EQ0−EQ7) possess only a lone pair of electrons, while thermodynamically the most unstable isomers EQ14−EQ16 possess three lone pairs of electrons.

Deduced from the structures and natural bond order (NBO) analysis, the isomers $CH_2CNH$ (EQ2) and $CH_2NCH$ (EQ5) can generally be considered as having a cumulenic structure,

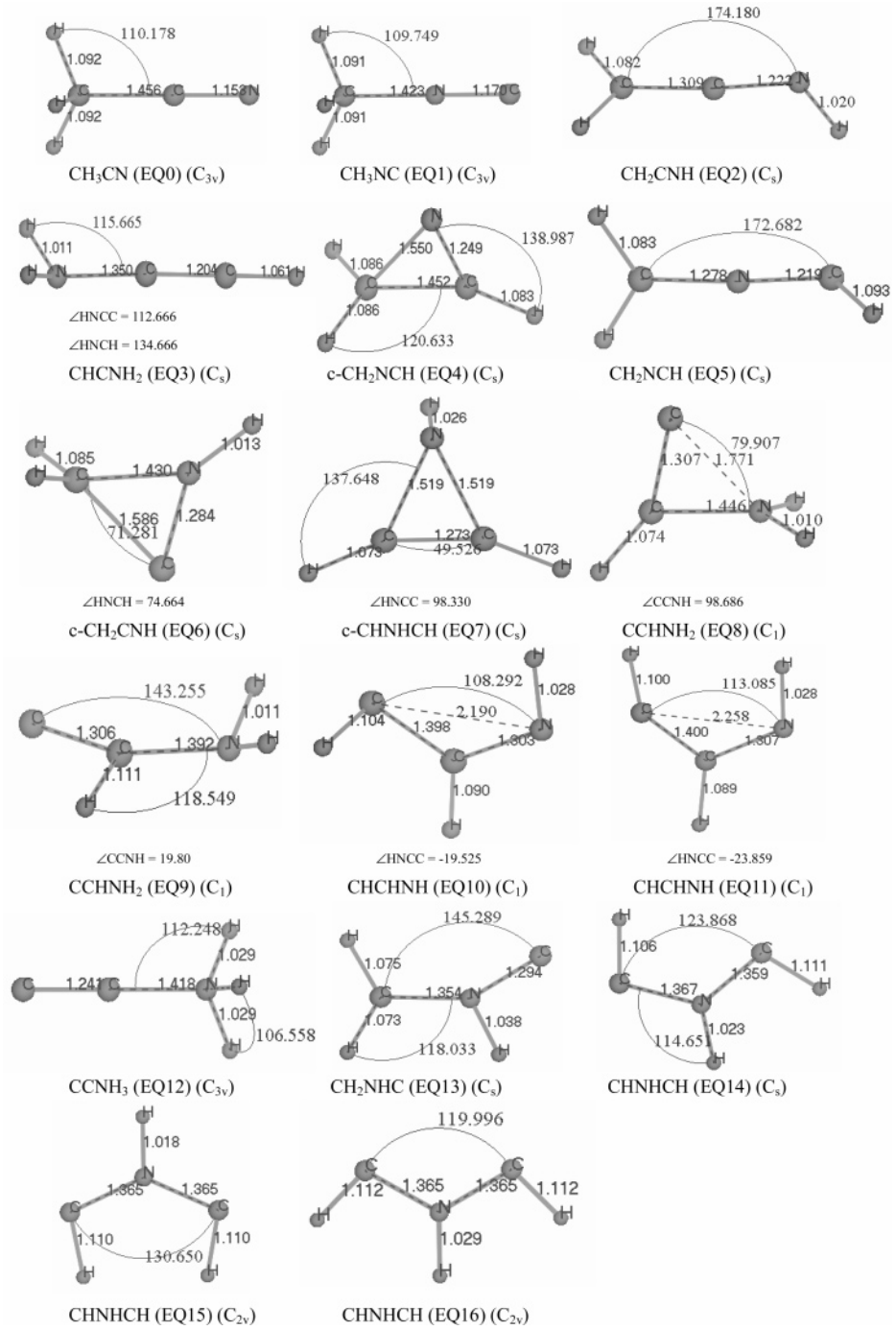


**Figure 1.** Optimized EQs found on the singlet potential energy surface for [$C_2$, $H_3$, N] isomers at the CCSD(T)/cc-pVTZ//DFT/B3LYP/6-311++G-(d,p) level. Bond lengths are in angstroms and angles in degrees.

HX═Y═$CH_2$, with $C_s$ symmetry, with X and Y being either a C or a N atom. The monohydrogenated X atom contains a lone pair of electrons. The internal Y atom is sp-hybridized. EQ2, which has a relative energy close to that of EQ1 (27.92 and 24.10 kcal/mol, respectively), is the third lowest lying [$C_2$, $H_3$, N] isomer. EQ5 contains the intramolecular donor−acceptor interaction between the N lone pair and vacant orbital of carbene. Adding the $^1NH_2$ radical directly to an ethyne molecule may possibly lead to the fourth most stable isomer $CHCNH_2$ (EQ3) with $C_s$ symmetry. Its strengthed C−N bond (length 1.35 Å, which is between the single and double CN bond lengths, 1.46 and 1.30 Å for single and double bonds, respectively) could be ascribed to the significant overlap between the lone pair orbital on the N atom and the $\pi$-orbital of the C≡C bond. Attaching $^1C_2$ to the $NH_3$ molecule can generate another chainlike high-energy (114.64 kcal/mol) isomer, $CCNH_3$ (EQ12), having $C_{3v}$ symmetry. This C−N single bond is formed when the lone pair orbital of $NH_3$ interacts with the CC vacant orbital. Thus, the CN bond structure in EQ12 contains a donor (N lone pair)−acceptor (C vacant orbital) bond character.

There are three thermodynamically stable cyclic isomers, c-$CH_2NCH$ (EQ4) (48.13 kcal/mol), c-$CH_2CNH$ (EQ6) (77.43 kcal/mol), and c-CHNHCH (EQ7) (81.83 kcal/mol), with CNC three-membered rings. EQ4 and EQ7 have the normal structure with $CH_2$ and NH taking a side addition to the C≡N bond of HCN and C≡C bond of acetylene $C_2H_2$, respectively. Interestingly, although EQ6 has a carbene structure, it is slightly lower in energy than EQ7. The lone pair of electrons on the N

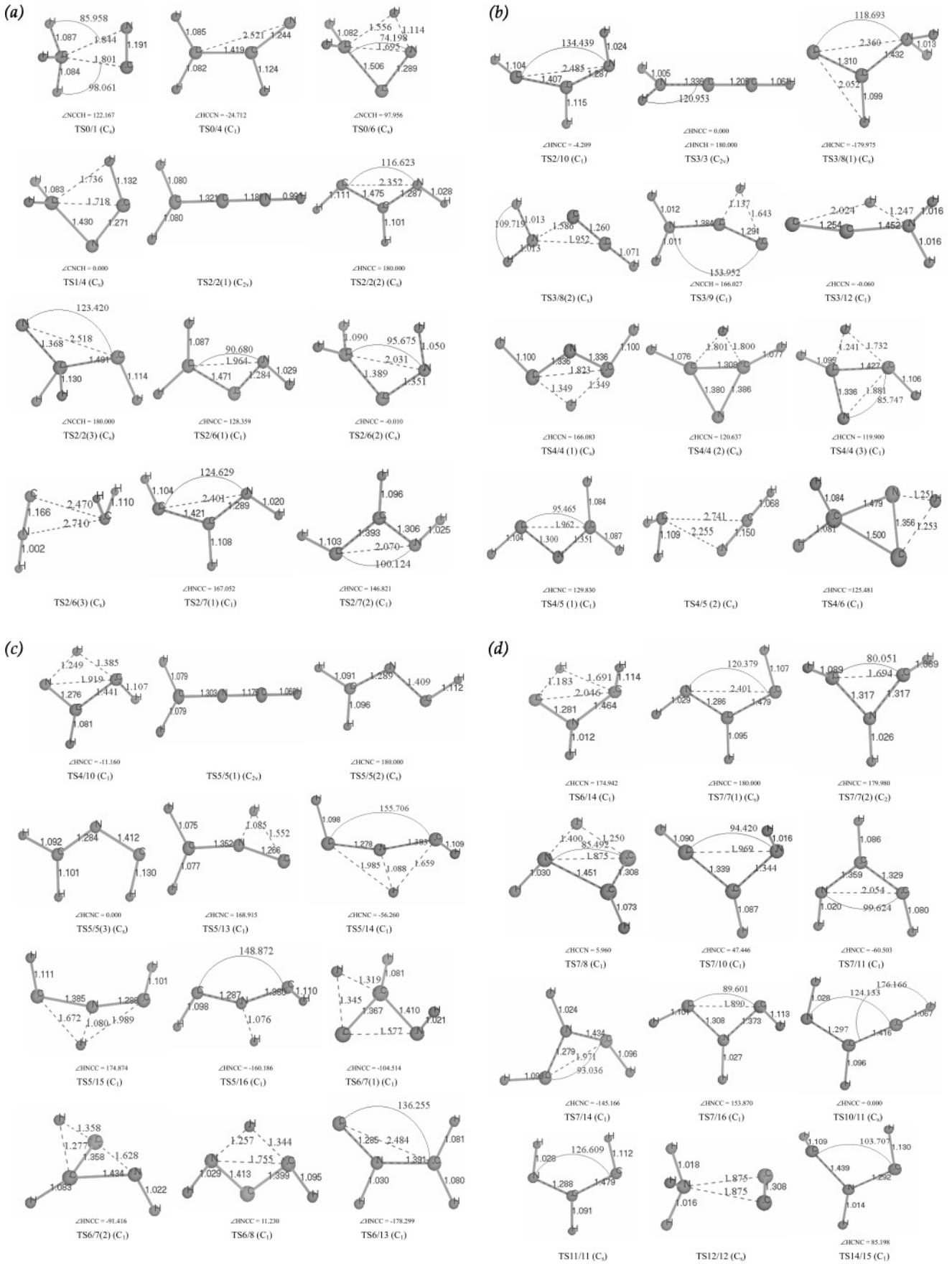


**Figure 2.** Optimized geometries of interconversion transition states between two EQs for singlet [$C_2$, $H_3$, N] isomers at the CCSD(T)/cc-pVTZ//DFT/B3LYP/6-311++G(d,p) level. Bond lengths are in angstroms and angles in degrees.

atom can effectively donate to the vacant orbital of the C atom, which greatly suppresses the carbene reactivity and increases the stability of EQ6. All the remaining acyclic bent isomers detected to present more than one lone pair of electrons are of

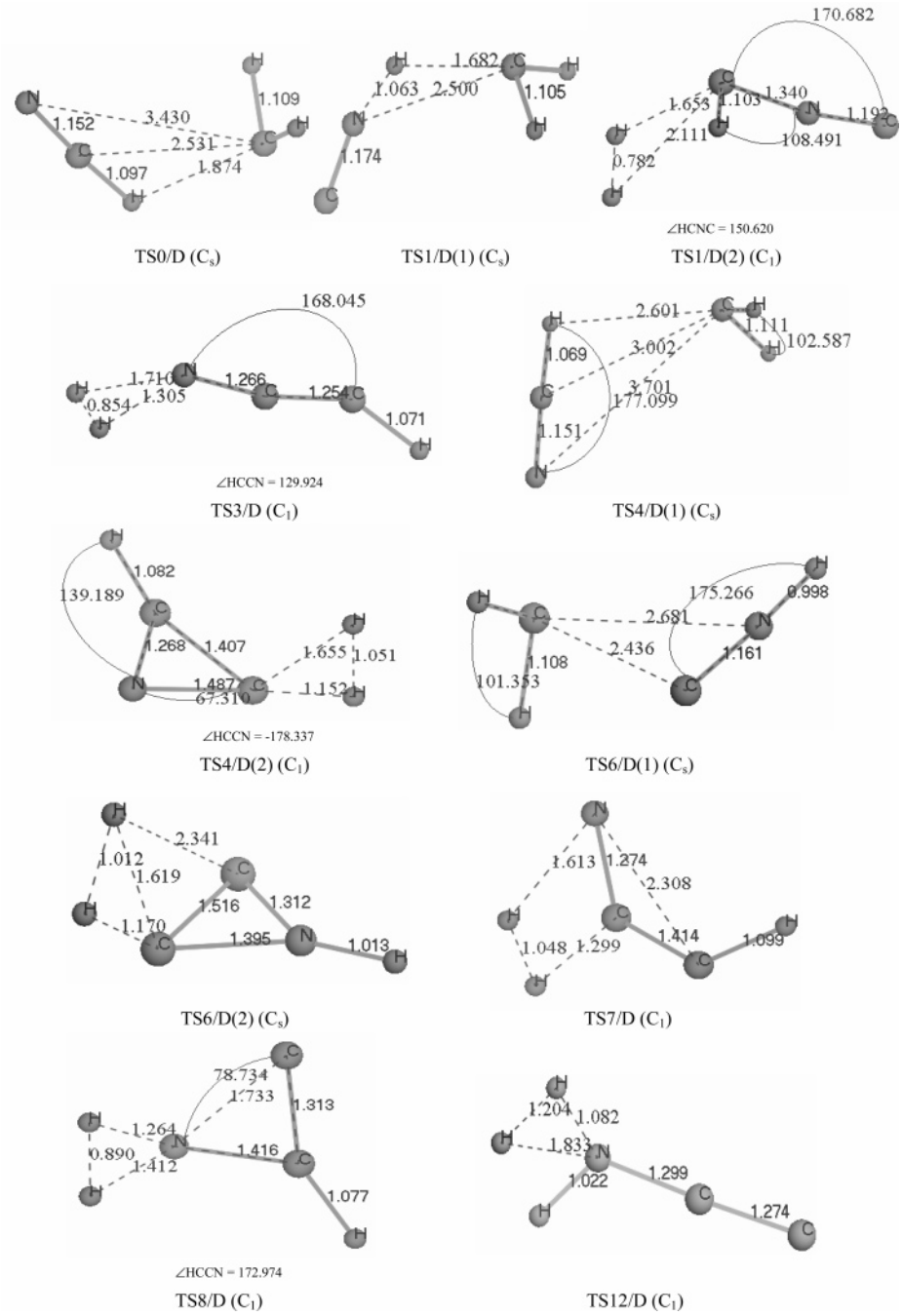


**Figure 3.** Optimized geometries of dissociation transition states found for singlet [$C_2$, $H_3$, N] isomers at the CCSD(T)/cc-pVTZ//DFT/B3LYP/6-311++G(d,p) level. Bond lengths are in angstroms and angles in degrees.

high thermodynamic instability according to the relative energy order. Among high-lying isomers, both EQ15 and EQ16 take on $C_{2v}$ symmetry. Apart from those structures with $C_s$ symmetry in the bent acyclic isomers, the remaining three isomers including EQ9, EQ10, and EQ11 possess $C_1$ symmetry. Among all found EQs, the geometries and order of stability for EQ0, EQ1, EQ2, EQ4, EQ5, EQ6, and EQ7 are in good agreement with previous results on cation.[18−24] Isomerization pathways for the neutral $CH_3CN$ are newly predicted except for the pathway between $CH_3CN$ and $CH_3NC$.

**3.2. Isomerization Pathways of $CH_3CN$.** The located transition states connecting the singlet [$C_2$, $H_3$, N] isomeric structures are displayed in Figure 2. Figure 5 illustrates the related potential energy diagram. The present SHS method gave three independent reaction paths starting from the most stable isomer EQ0 ($CH_3CN$) that directly or indirectly lead to the formation of three different cyclic isomers, EQ4, EQ6, and EQ7, respectively. Over subsequent energy barriers, the reaction paths starting from the three initial three-membered-ring products can lead to other intermediates and products. The total isomerization pathways were divided into three parts for clarity and convenience in the following discussion.

*Part I: Pathways from Acetonitrile EQ0 to the Cyclic Isomers c-$CH_2$NCH (EQ4), c-$CH_2$CNH (EQ6), and c-CHNHCH (EQ7).* EQ0 has a very high kinetic stability, with the lowest conversion barrier of 62.12 kcal/mol, governed by TS0/1. The reverse rearrangement from EQ1 to EQ0 is relatively easy with an energy barrier of 38.02 kcal/mol. With an activation energy of 63.37 kcal/mol, the H atom of the $CH_3$ group in EQ1 can transfer to the carbon of the CN group, as shown by TS1/4. The direct product is c-$CH_2$NCH (EQ4) with $C_s$ symmetry. The reverse reaction barrier is 39.34 kcal/mol. In addition to this,

**TABLE 1: Relative Energies (kcal/mol) of Various Singlet [$C_2$, $H_3$, N] Isomers and Isomerization and Dissociation Transition States at the DFT/B3LYP/6-311++G(d,p) and Single-Point CCSD(T)/cc-pVTZ//DFT/B3LYP/6-311++G(d,p) Levels with ZPE Correction**

| species | sym | ΔZPE, B3LYP/ 6-311++G(d,p) | B3LYP/ 6-311++G(d,p) + ZPE | CCSD(T)/ cc-pVTZ//DFT/ B3LYP/ 6-311++G(d,p) + ZPE | species | sym | ΔZPE, B3LYP/ 6-311++G(d,p) | B3LYP/ 6-311++G(d,p) + ZPE | CCSD(T)/ cc-pVTZ//DFT/ B3LYP/ 6-311++G(d,p) + ZPE |
|---|---|---|---|---|---|---|---|---|---|
| $CH_3CN$ (EQ0)[a] | $C_{3v}$ | 0.00 | 0.00 | 0.00 | TS4/5(1) | $C_1$ | −2.38 | 94.82 | 96.51 |
| $CH_3NC$ (EQ1) | $C_{3v}$ | −0.06 | 22.91 | 24.10 | TS4/5(2) | $C_s$ | −4.81 | 111.44 | 110.31 |
| $CH_2CNH$ (EQ2) | $C_s$ | −0.94 | 23.91 | 27.92 | TS4/6 | $C_1$ | −3.07 | 111.00 | 109.25 |
| $CHCNH_2$ (EQ3) | $C_s$ | −0.56 | 39.78 | 43.29 | TS4/10 | $C_1$ | −3.95 | 106.11 | 105.92 |
| c-$CH_2NCH$ (EQ4) | $C_s$ | −0.19 | 48.31 | 48.13 | TS5/5(1) | $C_{2v}$ | −2.50 | 61.62 | 69.05 |
| $CH_2NCH$ (EQ5) | $C_s$ | −1.44 | 51.39 | 57.10 | TS5/5(2) | $C_s$ | −2.57 | 100.65 | 103.41 |
| c-$CH_2CNH$ (EQ6) | $C_s$ | −0.56 | 76.62 | 77.43 | TS5/5(3) | $C_s$ | −4.40 | 107.30 | 107.93 |
| c-CHNHCH (EQ7) | $C_s$ | −1.00 | 81.26 | 81.83 | TS5/13 | $C_1$ | −3.28 | 122.86 | 126.06 |
| $CCHNH_2$ (EQ8) | $C_1$ | −0.38 | 88.48 | 90.23 | TS5/14 | $C_1$ | −3.26 | 147.02 | 150.90 |
| $CCHNH_2$ (EQ9) | $C_1$ | −1.63 | 89.04 | 91.87 | TS5/15 | $C_1$ | −4.02 | 148.84 | 149.03 |
| CHCHNH (EQ10) | $C_1$ | −2.07 | 96.45 | 99.22 | TS5/16 | $C_1$ | −4.39 | 144.95 | 148.71 |
| CHCHNH (EQ11) | $C_1$ | −1.88 | 97.89 | 99.77 | TS6/7(1) | $C_1$ | −3.40 | 126.12 | 126.38 |
| $CCNH_3$ (EQ12) | $C_{3v}$ | 0.50 | 112.76 | 114.64 | TS6/7(2) | $C_1$ | −3.14 | 128.63 | 128.63 |
| $CH_2NHC$ (EQ13) | $C_s$ | −2.06 | 121.92 | 125.31 | TS6/8 | $C_1$ | −4.39 | 136.80 | 137.42 |
| CHNHCH (EQ14) | $C_s$ | −1.75 | 125.88 | 128.20 | TS6/13 | $C_1$ | −2.51 | 125.36 | 125.36 |
| CHNHCH (EQ15) | $C_{2v}$ | −1.75 | 126.50 | 128.32 | TS6/14 | $C_1$ | −3.52 | 135.10 | 134.91 |
| CHNHCH (EQ16) | $C_{2v}$ | −2.07 | 130.14 | 132.40 | TS7/7(1) | $C_s$ | −2.07 | 104.86 | 105.80 |
| TS0/1 | $C_s$ | −1.25 | 62.75 | 62.12 | TS7/7(2) | $C_2$ | −3.10 | 141.31 | 139.24 |
| TS0/4 | $C_1$ | −3.14 | 95.38 | 90.99 | TS7/8 | $C_1$ | −3.38 | 115.33 | 113.26 |
| TS0/6 | $C_s$ | −3.57 | 102.28 | 101.53 | TS7/10 | $C_1$ | −2.38 | 97.80 | 100.52 |
| TS1/4 | $C_s$ | −2.88 | 89.17 | 87.47 | TS7/11 | $C_1$ | −2.63 | 99.89 | 103.47 |
| TS2/2(1) | $C_{2v}$ | −1.88 | 35.14 | 42.04 | TS7/14 | $C_1$ | −2.25 | 133.85 | 135.72 |
| TS2/2(2) | $C_s$ | −1.88 | 106.68 | 107.30 | TS7/16 | $C_1$ | −2.61 | 134.16 | 136.54 |
| TS2/2(3) | $C_s$ | −5.90 | 195.78 | 197.66 | TS10/11 | $C_s$ | −1.26 | 135.54 | 139.30 |
| TS2/6(1) | $C_1$ | −2.19 | 108.36 | 109.81 | TS11/11 | $C_s$ | −1.88 | 106.05 | 106.05 |
| TS2/6(2) | $C_s$ | −2.88 | 112.70 | 114.52 | TS12/12 | $C_s$ | −1.25 | 144.32 | 144.32 |
| TS2/6(3) | $C_s$ | −5.64 | 126.76 | 124.87 | TS14/15 | $C_1$ | −3.01 | 136.10 | 136.60 |
| TS2/7(1) | $C_1$ | −2.51 | 99.77 | 103.53 | TS0/D | $C_s$ | −3.02 | 109.20 | 108.00 |
| TS2/7(2) | $C_1$ | −2.51 | 101.66 | 105.42 | TS1/D(1) | $C_s$ | −1.28 | 123.55 | 124.50 |
| TS2/10 | $C_1$ | −2.76 | 97.40 | 99.60 | TS1/D(2) | $C_1$ | −6.10 | 120.35 | 124.68 |
| TS3/3 | $C_{2v}$ | −1.25 | 40.16 | 43.92 | TS3/D | $C_1$ | −1.30 | 129.83 | 138.80 |
| TS3/8(1) | $C_s$ | −1.88 | 93.50 | 95.38 | TS4/D(1) | $C_s$ | −5.21 | 112.51 | 110.62 |
| TS3/8(2) | $C_s$ | −1.88 | 111.70 | 114.83 | TS4/D(2) | $C_1$ | −5.69 | 136.00 | 136.98 |
| TS3/9 | $C_1$ | −1.88 | 90.48 | 92.98 | TS6/D(1) | $C_s$ | −5.08 | 126.63 | 125.06 |
| TS3/12 | $C_1$ | −3.01 | 140.06 | 143.20 | TS6/D(2) | $C_s$ | −2.00 | 164.22 | 165.91 |
| TS4/4(1) | $C_s$ | −4.39 | 116.72 | 117.97 | TS7/D | $C_1$ | −7.50 | 188.87 | 192.64 |
| TS4/4(2) | $C_s$ | −4.80 | 142.56 | 144.33 | TS8/D | $C_1$ | −6.11 | 167.54 | 170.49 |
| TS4/4(3) | $C_1$ | −4.22 | 168.55 | 172.62 | TS12/D | $C_1$ | −2.66 | 167.73 | 169.24 |

[a] All values are calculated with regard to the isomer EQ0 for which the total energies are −132.7528525 and −132.4842687 au at the B3LYP/6-311++G(d,p) and single-point CCSD(T)/cc-pVTZ//DFT/B3LYP/6-311++G(d,p) levels, respectively. The ZPE of the EQ0 at the B3LYP/6-311++G(d,p) level is 0.043348 au.

there exist two competitive single-step reaction channels from EQ0 to cyclic isomers. One is a rearrangement of $CH_3CN$ to c-$CH_2NCH$ that occurs by a direct 1,2-hydrogen transfer via TS0/4. The TS0/4 is nonplanar with a NCC angle of 156.8°. The barrier height for the $CH_3CN$ (EQ0) → c-$CH_2NCH$ (EQ4) reaction is 90.99 kcal/mol, and that for the reverse process is calculated as 42.86 kcal/mol. The other is through a direct 1,3-hydrogen shift, from C to N, with an activation energy of 101.53 kcal/mol via the product-like TS0/6 of $C_s$ symmetry to give c-$CH_2CNH$ (EQ6) possessing $C_s$ symmetry, similar to 1,3-hydrogen transfer from EQ1 to EQ4. The reaction coordinate involves the deformation of the chainlike skeleton, leading to the C−N bond formation and a ring closure. The barrier for the reverse route is only 24.10 kcal/mol. It is obvious that both the two lowest energy species EQ0 and EQ1 can rearrange endothermically to form the cyclic c-$CH_2NCH$ (EQ4), which is the most stable among the three monocyclic singlet isomers. As Figure 5 shows, the cyclic isomers c-$CH_2NCH$ (EQ4) and c-$CH_2CNH$ (EQ6) can isomerize further via endothermic or exothermic channels to lead to another higher lying cyclic structure, c-CHNHCH (EQ7), which will be discussed in Part II.

*Part II: Interconversion between Cyclic Isomers.* The most direct isomerization among three-memebered-ring isomers occurs through the successive H-hopping pathway EQ4 ↔ EQ6 ↔ EQ7 and involves the cyclic TS4/6 and ringlike TS6/7(1)// TS6/7(2) lying at 109.25 and 126.38/128.63 kcal/mol, respectively. The H atom takes the intermediate position between the N and C atoms at the first transition state TS4/6, and prefers to be close to hydrogenated carbon at transition states TS6/7(1)// TS6/7(2) for the conversion between EQ6 and EQ7 (Figure 2). Both the TS6/7(1) and TS6/7(2) have $C_1$ symmetry with the nearly formed CCN ring and the separated H atom positioned almost perpendicularly to the CCN plane. The rearrangement for the route EQ7 → EQ6 → EQ4 is relatively easy with activation energies of 31.82 and 44.55 kcal/mol, respectively. Alternatively, with an activation barrier of 18.69 kcal/mol, c-CHNHCH (EQ7) can be activated to an acyclic transition state, TS7/10, in which C−N bond is broken due to its strong stretching motion, leading to a kinetically unstable acyclic

**TABLE 2: Relative Energies (kcal/mol) of the Dissociation Products of [$C_2$, $H_3$, N] Isomers and Energy Barriers for the Possible Dissociation Channels at the DFT/B3LYP/6-311++G(d,p) and Single-Point CCSD(T)/cc-pVTZ//DFT/B3LYP/6-311++G(d,p) Levels**[a]

| | relative energy of the products | | dissociation energy barrier | |
|---|---|---|---|---|
| dissociation channel (DC) | B3LYP/6-311++G(d,p) | CCSD(T)/cc-pVTZ//DFT | B3LYP/6-311++G(d,p) | CCSD(T)/cc-pVTZ//DFT |
| $CH_3CN$ (EQ0) → $CH_3$ ($^2A_2''$) + CN ($^2\Sigma^+$)[b] | 96.00 | 109.18 | 96.00 | 109.18 |
| $CH_3CN$ (EQ0) → $CH_2$ ($^1A_1$) + HCN ($^1\Sigma^+$) | 96.38 | 97.64 | 109.20 | 108.00 |
| c-$CH_2NCH$ (EQ4) → $CH_2$ ($^1A_1$) + HCN ($^1\Sigma^+$) | 96.38 | 97.64 | 64.20 | 62.49 |
| $CH_3NC$ (EQ1) → $CH_2$ ($^1A_1$) + HNC ($^1\Sigma^+$) | 106.28 | 111.50 | 100.64 | 100.40 |
| c-$CH_2CNH$ (EQ6) → $CH_2$ ($^1A_1$) + HNC ($^1\Sigma^+$) | 106.28 | 111.50 | 50.01 | 47.63 |
| c-$CH_2CNH$ (EQ6) → c-CCNH ($^1A'$) + $H_2$ ($^1\Sigma_g^+$) | 114.83 | 113.66 | 87.60 | 88.48 |
| c-$CH_2NCH$ (EQ4) → c-CNCH ($^1A'$) + $H_2$ ($^1\Sigma_g^+$) | 102.28 | 104.11 | 87.69 | 88.85 |
| $CCHNH_2$ (EQ8) → c-CNCH ($^1A'$) + $H_2$ ($^1\Sigma_g^+$) | 102.28 | 104.11 | 79.06 | 80.26 |
| $CH_3NC$ (EQ1) → CNCH ($^1A'$) + $H_2$ ($^1\Sigma_g^+$) | 108.56 | 110.80 | 97.44 | 100.58 |
| $CHCNH_2$ (EQ3) → NCCH ($^1A'$) + $H_2$ ($^1\Sigma_g^+$) | 83.46 | 84.10 | 90.05 | 95.51 |
| c-CHNHCH (EQ7) → NCCH ($^1A'$) + $H_2$ ($^1\Sigma_g^+$) | 83.46 | 84.10 | 107.61 | 110.81 |
| $CCNH_3$ (EQ12) → CCNH ($^1\Sigma^+$) + $H_2$ ($^1\Sigma_g^+$) | 127.38 | 128.60 | 54.97 | 54.60 |
| c-CHNHCH (EQ7) → NH ($^1\Sigma^+$) + CHCH ($^1\Sigma_g^+$)[b] | 146.21 | 149.32 | 64.95 | 67.49 |

[a] The total energies of the reference isomer EQ0 at the DFT/B3LYP/6-311++G(d,p) and single-point CCSD(T)/cc-pVTZ//DFT/B3LYP/6-311++G(d,p) levels as well as the ZPE at the DFT/B3LYP/6-311++G(d,p) level are listed in footnote *a* of Table 1. [b] Dissociation channels without a TS.

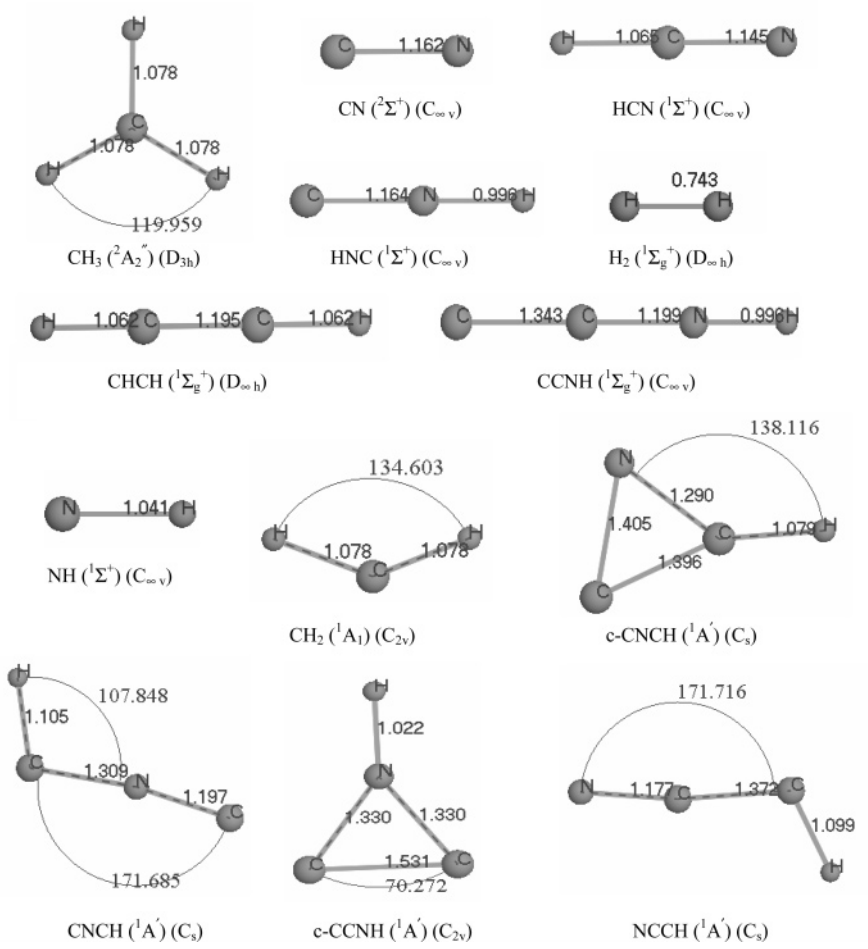


**Figure 4.** Optimized geometries of dissociation products found on the singlet potential energy surface at the CCSD(T)/cc-pVTZ//DFT/B3LYP/6-311++G(d,p) level. Bond lengths are in angstroms and angles in degrees.

isomer, EQ10. The path EQ10 → cyclic EQ4 seems energetically possible and kinetically fast since the activation barrier is only 6.70 kcal/mol via TS4/10. However, 1,2-H shift from EQ10 to EQ2 would be extremely fast because the corresponding movement occurs with an energetic cost of only 0.38 kcal/mol.

Isomerizing from EQ4 to other two cyclic isomers, three competitive three-step reaction channels and a two-step reaction mechanism exist. The first channel leads back to EQ1 via an acyclic transition state, TS1/4, with $C_s$ symmetry. This feasible pathway is EQ4 → EQ1 → EQ0 → EQ6. The activation energies are 39.34, 40.06, and 101.53 kcal/mol for the three steps, respectively. The activation barriers of the counterreaction EQ6 → EQ0 → EQ1 → EQ4 are 24.10, 64.16, and 63.37 kcal/mol for each step, respectively, implying that the reverse reaction seems to be favorable. The second three-step process involves the breaking of a C−C bond in the three-membered ring from

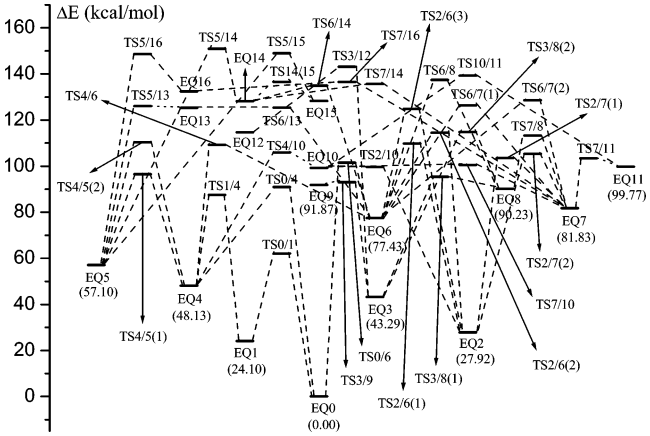


**Figure 5.** Energetic profile (kcal/mol) of the potential energy surface for isomerization pathways of singlet [$C_2$, $H_3$, N] isomers at the CCSD(T)/cc-pVTZ//DFT/B3LYP/6-311++G(d,p) level.

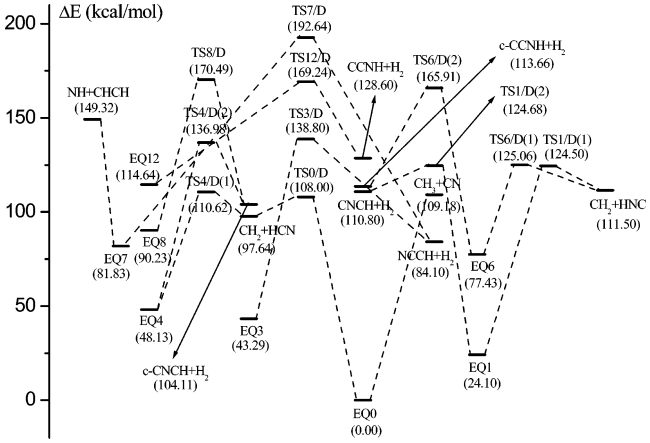


**Figure 6.** Energetic profile (kcal/mol) of the potential energy surface for dissociation channels of singlet [$C_2$, $H_3$, N] isomers at the CCSD(T)/cc-pVTZ//DFT/B3LYP/6-311++G(d,p) level.

EQ4 to EQ5 and a proton-transfer process from EQ5 to EQ14, eventually resulting in the formation of cyclic isomers EQ6 and EQ7 with small energy barriers of 6.71 and 7.52 kcal/mol for the last step, respectively. The lowest energy barrier, which controls the kinetic stability of the isomers, is 48.38 kcal/mol for the first step, EQ4 → EQ5, and 93.80 kcal/mol for the second step, EQ5 → EQ14. Another high-lying transition state, TS4/5(2), 110.31 kcal/mol above the global minimum in the EQ4 → EQ5 conversion involves the breaking of two bonds, C−C and C−N, in the three-membered ring, as shown in Figure 2. The third indirect path involves the formation of kinetically unstable intermediate EQ13 via TS5/13 with an energy of 68.96 kcal/mol with respect to EQ5, resulting in an instantaneous formation of the product EQ6 because of a very small barrier of 0.05 kcal/mol via TS6/13. The two-step mechanism also leads back to the most stable isomer, EQ0, over the barrier of 42.86 kcal/mol, followed by TS0/6, as mentioned above, producing cyclic EQ6.

Over a conversion barrier of 32.38 kcal/mol, the single C−N bond in EQ6 can break to form the stable cumulenic structure EQ2. Starting from EQ2, over an energy barrier of 71.68 kcal/mol, 1,2-hydrogen migration happens from the methylene hydrogen to the intermediate carbon, as shown by TS2/10, resulting in EQ10 and then easier conversion to c-CHNHCH (EQ7) (the energy barrier is only 1.30 kcal/mol). If the energy of the system EQ2 reaches 103.53 kcal/mol relative to that of the initial stage EQ0, EQ2 can directly convert to cyclic isomer c-CHNHCH (EQ7) by 1,2-H shift without any other intermediate. This isomerization process has another transition state, TS2/7(2) (105.42 kcal/mol), structurally and energetically close to TS2/7(1), as shown by Figure 2. Their activation barriers are 75.61 and 77.50 kcal/mol, respectively. It is worthwhile to note that the conversion barrier of EQ2 → EQ6 is only 6.28 kcal/mol higher than that of EQ2 → EQ7, indicating that two kinds of reactions are competitive. If the energy of the system is higher by 59.99 kcal/mol than that of EQ6, EQ8 with $C_1$ symmetry can be produced through 1,2-H transfer from C to N and the broken double C═N bond in cyclic EQ6, followed by TS7/8 with an activation of 23.03 kcal/mol, leading to another cyclic isomer, EQ7, by a continuous 1,2-H shift from N to C.

*Part III: Isomerization from Cyclic Isomers to Acyclic Isomers.* The thermodynamically stable cyclic isomer c-$CH_2NCH$ (EQ4) can convert into very stable acetonitrile EQ0, methyl isocyanide EQ1, and metastable intermediate EQ5, which is exothermic by 48.13 and 24.03 kcal/mol for EQ0 and EQ1, respectively, and endothermic by 8.97 kcal/mol for EQ5. Starting from EQ5, isomerization reaction can continue to take place to form higher energy acyclic isomers EQ13, EQ14, EQ15, and EQ16 with corresponding energy barriers of 68.96, 93.80, 91.93, and 91.61 kcal/mol, respectively. However, the 1,2-H migration process from EQ13 to EQ5 occurs more easily because of a very small conversion barrier of 0.75 kcal/mol. The isomers EQ14 and EQ15 lie not only energetically very close (an energy difference of 0.12 kcal/mol), but also can be transformed into each other very easily (the barrier height is 8.40 kcal/mol from EQ14 to EQ15 and 8.28 kcal/mol for the reverse process). Alternatively, EQ4 can directly rearrange to high-lying acyclic isomer EQ10 with an activation barrier of 57.79 kcal/mol. Also, the reverse rearrangements from these high-lying acyclic isomers proceed very easily only within an energy barrier range of 0.75−22.70 kcal/mol. It is obvious that these thermodynamically unstable acyclic isomers could also be considered as kinetically unstable. Especially, high-lying acyclic species EQ10, EQ13, and EQ14 reside in a very shallow potential well with their respective lowest barriers at 0.38 (EQ10 → EQ2), 0.05 (EQ13 → EQ6), and 6.71 (EQ14 → EQ6) kcal/mol. These low barriers do not ensure their kinetic stability in the gas phase, indicating their transient nature.

The opening of c-$CH_2CNH$ (EQ6) to acetonitrile EQ0 can be accomplished via TS0/6 with a conversion barrier of 24.10 kcal/mol, as mentioned above. Another ring-opening method of converting EQ6 into more stable chainlike $CH_2CNH$ (EQ2) is through transition state TS2/6(1)//TS2/6(2)//TS2/6(3) lying 32.38//37.09//47.44 kcal/mol higher than c-$CH_2CNH$ (EQ6). In addition, EQ6 can also be converted into higher lying acyclic isomers EQ8, EQ13, and EQ14 owing to H migration and the opening of the three-membered ring. Acyclic isomerization would be further accomplished. Starting from EQ8, a 1,2-hydrogen shift mechanism can occur from the hydrogen of the medial carbon atom to the terminal carbon atom due to a small activation energy of 5.15 kcal/mol with chainlike $CHCNH_2$ (EQ3) as a stable intermediate, eventually leading to the formation of the isomers $CCHNH_2$ (EQ9) with $C_1$ symmetry and $CCNH_3$ (EQ12) with $C_{3v}$ symmetry (lying 91.87 and 114.64 kcal/mol above the global minimum, respectively). Metastable cyclic isomer EQ7, in a similar interconversion method with EQ14, can rearrange endothermically to another high-lying acyclic isomer, EQ16, with an activation energy of 54.71 kcal/mol via TS7/16, where its barrier is only 0.82 kcal/mol higher than that of the reaction EQ7 → EQ14, indicating that the two kinds of conversion from EQ7 to high-energy isomers

are competitive. Over a conversion barrier of 31.43 kcal/mol, c-CHNHCH (EQ7) can be favorable to rearrange to more stable EQ2 and high-lying isomers EQ8, EQ10, and EQ11. The reverse barriers for higher lying species are only 1.30−23.03 kcal/mol.

Several degenerate rearrangements proceed with the lowest energetic barriers of 0.63−69.84 kcal/mol, such as EQ2 ↔ EQ2 via TS2/2(1) with $C_{2v}$ symmetry (an activation barrier of 14.12 kcal/mol) where the H atom at nitrogen remains linear with the CCN skeleton, EQ3 ↔ EQ3 via TS3/3 (an activation barrier of 0.63 kcal/mol) with $C_{2v}$ symmetry, different from the $C_s$ symmetry of EQ3, although their geometries are similar, EQ4 ↔ EQ4 via TS4/4(1) with $C_s$ symmetry (an activation barrier of 69.84 kcal/mol) in which the H atom resides in the meso position between two carbon atoms, EQ5 ↔ EQ5 via TS5/5(1) (an activation barrier of 11.95 kcal/mol) where the H atom locates at a linear position in the CNCH bond structure, resulting in $C_{2v}$ symmetry, EQ7 ↔ EQ7 via TS7/7(1) with $C_s$ symmetry (an activation barrier of 23.97 kcal/mol) in which the three-membered ring breaks at the C−N bond, EQ11 ↔ EQ11 via TS11/11 with $C_s$ symmetry (an activation barrier of 6.28 kcal/mol), the structure of which is close to that of the product EQ11, and EQ12 ↔ EQ12 via TS12/12 with $C_s$ symmetry (an activation barrier of 29.68 kcal/mol) where two-body dissociation arises from breaking of the single C−N bond, as shown in Figure 2. Besides these lower energy transition states that govern the kinetic stability of the degenerate rearrangements, the higher energy TS2/2(2)//TS2/2(3), TS4/4(2)//TS4/4(3), TS5/5(2)//TS5/5(3), and TS7/7(2) of $C_2$ symmetry with barrier energies of 79.38//169.14, 96.20//124.49, 46.31//50.83, and 57.41 kcal/mol, respectively, can also be confirmed by IRC calculations. Their structure parameters are displayed in Figure 2.

**3.3. Dissociation Channels (DCs) of [$C_2$, $H_3$, N] Isomers.** Traces by the SHS algorithm revealed 11 DCs with TSs including CC bond dissociation and the hydrogen abstraction and migration of [$C_2$, $H_3$, N] isomers. The corresponding transition states (TS*n*/D(*i*)) and dissociation fragments are presented in Figures 3 and 4, respectively. The obtained values of the dissociation barriers and relative energies of the products including two DCs without TSs are summarized in Table 2, while Figure 6 shows the related energy diagram.

As can be seen from Table 2 and Figure 6, the most stable isomer EQ0 can directly dissociate into $CH_3$ ($^2A_2''$) and CN ($^2\Sigma^+$) radicals without the corresponding transition state detected, which is an energy-increasing process. The $CH_3$ ($^2A_2''$) + CN ($^2\Sigma^+$) dissociation fragments lie 109.18 kcal/mol above the global minimum EQ0. Providing 108.00 kcal/mol energy to EQ0, $CH_3CN$ dissociates into $CH_2$ ($^1A_1$) + HCN ($^1\Sigma^+$) via the migration of one of the H atoms of the methyl group onto the adjacent C atom, in which the breaking CC bond in TS0/D is elongated by up to 0.67 Å. It is obvious that this decomposition is a strong competitive reaction relative to the direct CC bond dissociation of acetonitrile because of a very close energy barrier for two kinds of dissociation processes (a difference of only 1.18 kcal/mol). Another way to produce $^1CH_2$ and HCN is through the CC and CN bond scission of cyclic intermediate EQ4 via TS4/D(1) with a barrier height of 62.49 kcal/mol. Alternatively, $^1CH_2$ can be obtained through other two paths which lead to the same dissociation products—$CH_2$ ($^1A_1$) + HNC ($^1\Sigma^+$). In one path the H atom of the methyl group can shift to the neighbor nitrogen atom with an activation barrier of 100.40 kcal/mol via TS1/D(1), resulting in the formation of the $CH_2$ ($^1A_1$) and HNC ($^1\Sigma^+$) molecules, similar to the dissociation mechanism of EQ0 → $CH_2$ ($^1A_1$) + HCN ($^1\Sigma^+$). The second path take place apparently resulting from a strong strain in the three-membered-ring EQ6 via TS6/D(1) with an energy barrier of 47.63 kcal/mol. When the C atom connecting two H atoms is expelled from the three-membered ring on account of its $sp^3$ hybrid character, both the C−C and C−N bonds are broken, but another C−N bond is strengthened to yield a HNC ($^1\Sigma^+$) molecule. The HNC structure in TS6/D(1) is very close to linear.

Raising the system EQ6's energy to a higher level, a hydrogen abstraction pathway becomes probable. As shown by TS6/D(2) with $C_s$ symmetry, when two H atoms separate from the bonded carbon atom, single C−C and C−N bonds become shorter and the double C═N bond lengthens by 0.03 Å. The barrier height for the $H_2$ elimination is 88.48 kcal/mol. However, it may be important to note that the dissociation bimolecular complex $H_2$ ($^1\Sigma_g^+$) + c-CCNH ($^1A'$) is of kinetic stability since its association reaction is more energy demanding (an energy barrier of 52.25 kcal/mol) with respect to other dissociation fragments mentioned above (within a range of the barrier height of 10.36−13.56 kcal/mol for the reverse association processes). Delocalization of the lone electron pairs on two carbon atoms to three-membered-ring c-CCNH is a main factor in increasing the stability for the fragment molecule. Similarly, both cyclic isomer EQ4 and acyclic isomer EQ8 can abstract two hydrogen atoms from respective $CH_2$ and $NH_2$ groups as a result of strong $CH_2$ and $NH_2$ rocking modes, leading to the formation of $H_2$ and c-CNCH ($^1A'$) with $C_s$ symmetry. The individual barrier heights are 88.85 and 80.26 kcal/mol via TS4/D(2) and TS8/D, respectively. Compared with the geometrical parameters of reactant EQ8, the C−N bond is shortened into double character and the C−C bond is stretched into a single bond in c-CNCH. It is possible to obtain the same $H_2$ dissociation product when starting from four different initial stage isomers, EQ1, EQ3, EQ7, and EQ12, via TS1/D(2), TS3/D, TS7/D, and TS12/D, respectively. All four isomers can break the hydrogenation bonds down into two hydrogen atoms for the formation of a hydrogen molecule, leaving a chainlike NCC or CNC skeleton bonded with one hydrogen atom. The hydrogen elimination in EQ1 is a competitive process with reference to its dissociation EQ1 → $CH_2$ ($^1A_1$) + HNC ($^1\Sigma^+$) involving the transfer of a H atom. Their energy barrier difference is only 0.18 kcal/mol. The hydrogen abstractions in the dissociation channels of EQ3 and EQ12 are derived from the coupled motion of CCN framework stretching and NH rocking, resulting in $H_2$ ($^1\Sigma_g^+$) + NCCH ($^1A'$) and $H_2$ ($^1\Sigma_g^+$) + CCNH ($^1\Sigma^+$), respectively. Moreover, these two kinds of dissociation products are of relatively high kinetic stability with a reverse association barrier of 54.70 kcal/mol for EQ3 and 40.64 kcal/mol for EQ12. The hydrogen elimination process in cyclic EQ7 is owed to the strain of the three-membered ring and largely a C−N stretching motion, leading to a cleaved C−N bond of 2.31 Å and a N−C−C orientation angle of 158.62° as well as a hydrogen molecule, which is more energy demanding than the available DC for the formation of NH ($^1\Sigma^+$) and acetylene $C_2H_2$ ($^1\Sigma_g^+$) starting from EQ7. The dissociation energy barriers are 110.81 and 67.49 kcal/mol, respectively.

It is evident that the chance of possible hydrogen migration pathways along the CCN skeleton is significantly probable with respect to direct CC bond dissociation of $CH_3CN$ from our theoretical calculation, indicating the existence of a hydrogen migration process or CCN skeletal rearrangements occurring prior to direct dissociation.

## 4. Conclusions

The pathways around the equilibrium structure $CH_3CN$ can be discovered by the SHS method, which enables us to make a

global analysis of the potential energy surface for a given chemical composition in combination with a downhill-walk algorithm. Total reaction pathways including all transition states, dissociation channels, and equilibrium structures were obtained for an ab initio singlet PES at the CCSD(T)/cc-pVTZ//DFT/B3LYP/6-311++G(d,p) level. Our calculations have revealed 17 equilibrium structures, 59 transition states, and 13 dissociation channels on the singlet PES. Those isomers with thermodynamic stability are also found to be kinetically stable. The acetonitrile EQ0 is the most stable isomer and global minimum followed by three other chainlike isomers, $CH_3NC$ (EQ1), $CH_2CNH$ (EQ2), and $CHCNH_2$ (EQ3), in which the lowest conversion barriers are predicted to be within a range of 49.69−101.53 kcal/mol. Three-membered-ring isomers c-$CH_2NCH$ (EQ4), c-$CH_2CNH$ (EQ6), and c-CHNHCH (EQ7) can be considered as metastable intermediates which can further convert into the low-lying chainlike isomers and higher lying acyclic isomers with the lowest conversion barriers of 21.70−59.99 kcal/mol.

Possible routes for isomerization and dissociation have been identified on both PESs. Interconversion between acetonitrile ($CH_3CN$) and methyl isocyanide ($CH_3NC$) can occur via direct CC bond dissociation transition states (TS0/1) located 62.12 kcal/mol above the global minimum. The stable chainlike isomers are subject to high barriers toward isomerization to other isomers. Acylic high-lying isomers not only lie energetically close but also can be converted to each other easily. Moreover, they can easily rearrange to the cyclic isomers. Radiation may lead to the dissociation of the initial singlet $CH_3CN$ molecule, and the recombination of the resultant radicals can produce new isomers, which may further dissociate or isomerize to energetically more favorable channels. The 13 DCs revealed have implied that the chance of H shift and deformation of the CCN skeleton is significantly probable relative to direct CC bond dissociation of $CH_3CN$, in which an attempt has been undertaken to indicate a plausible explanation for the hydrogen atom migration proceeding in competition with the direct CC bond dissociation, even prior to the dissociation. Now, most transition states and interconversion pathways for the neutral $CH_3CN$ are predicted for the first time, which should be helpful for future identification of these [$C_2$, $H_3$, N] isomers in both the laboratory and interstellar space.

**Acknowledgment.** The present work was partially supported by the Ministry of Education, Culture, Sports, Science and Technology via a Grant-in-Aid for the COE project Giant Molecules and Complex Systems. S.M. is supported by a Research Fellowship of the Japan Society for the Promotion of Science for Young Scientists.

## References and Notes

(1) Hamm, S.; Warneck, P. *J. Geophys. Res.* **1990**, *95*, 20593.
(2) Brasseur, G.; Arijs, E.; De Rudder, A.; Nevejans, D.; Angels, *J. Geophys. Res. Lett.* **1983**, *10*, 725.
(3) Tyndall, G. S.; Orlando, J. J.; Wallington, T. J.; Sehested, J.; Nielsen, O. J. *J. Phys. Chem.* **1996**, *100*, 660 and references therein.
(4) Watanabe, M.; Hirakoso, H.; Sawamoto, S.; Adschiri, T.; Arai, K. *J. Supercrit. Fluids* **1998**, *13*, 247.
(5) Sasaki, M.; Kabyemela, B.; Malaluan, R.; Hirose, S.; Takeda, N.; Adschiri, T.; Arai, K. *J. Supercrit. Fluids* **1998**, *13*, 261.
(6) Yoshida, H.; Terashima, M.; Takahashi, Y. *Biotechnol. Prog.* **1999**, *15*, 1090.
(7) Quitain, A. T.; Faisal, M.; Kang, K.; Daimon, H.; Fujie, K. *J. Hazard. Mater.* **2002**, *B93*, 209.
(8) Ashfold, M. N. R.; Simons, J. P. *J. Chem. Soc., Faraday Trans. 2* **1978**, *174*, 1263.
(9) Hynes, A. J.; Wine, P. H. *J. Phys. Chem.* **1991**, *95*, 1232.
(10) Budge, S.; Roscoe, J. M. *Can. J. Chem.* **1995**, *73*, 666.
(11) Moriyama, M.; Tsutsui, Y.; Honma, K. *J. Chem. Phys.* **1998**, *108*, 6215.
(12) Li, Q.-S.; Wang, C.-Y. *J. Phys. Chem. A* **2002**, *106*, 8883.
(13) Wang, B.; Hou, H.; Gu, Y. *J. Phys. Chem. A* **2001**, *105*, 156.
(14) Lindstedt, P. R. *Proc. Combust. Inst.* **1998**, 20.
(15) Richter, H.; Howard, J. B. *Prog. Energy Combust. Sci.* **2000**, *26*, 565.
(16) Dollet, A. *Surf. Coat. Technol.* **2004**, *177*, 245.
(17) Hishikawa, A.; Hasegawa, H.; Yamanouchi, K. *J. Electron Spectrosc. Relat. Phenom.* **2004**, *141*, 195.
(18) Choe, J. C. *Int. J. Mass Spectrom.* **2004**, *235*, 15.
(19) van Thuijl, J.; van Houte, J. J.; Maquestiau, A.; Flammang, R.; DeMeyer, C. *Org. Mass Spectrom.* **1977**, *12*, 196.
(20) Chess, E. K.; Lapp, R. L.; Gross, M. L. *Org. Mass Spectrom.* **1982**, *17*, 475.
(21) Marotta, E.; Traldi, P. *Rapid Commun. Mass Spectrom.* **2003**, *17*, 2846.
(22) Swanton, D. J.; Bacskay, G. B.; Willett, G. D.; Hush, N. S. *J. Mol. Struct.: THEOCHEM* **1983**, *91*, 313.
(23) Harland, P. W.; Maclagan, R. G. A. R.; Schaefer, H. F. *J. Chem. Soc., Faraday Trans. 2* **1989**, *85*, 187.
(24) Mayer, P. M.; Taylor, M. S.; Wong, M. W.; Radom, L. *J. Phys. Chem. A* **1998**, *102*, 7074.
(25) Ohno, K.; Maeda, S. *Chem. Phys. Lett.* **2004**, *384*, 277.
(26) Maeda, S.; Ohno, K. *J. Phys. Chem. A* **2005**, *109*, 5742.
(27) Maeda, S.; Ohno, K. *Chem. Lett.* **2004**, *33*, 1372.
(28) Maeda, S.; Ohno, K. *Chem. Phys. Lett.* **2004**, *398*, 240.
(29) Maeda, S.; Ohno, K. *Chem. Phys. Lett.* **2005**, *404*, 95.
(30) Fukui, K. *Acc. Chem. Res.* **1981**, *14*, 363.
(31) Page, M.; Mclver, J. W., Jr. *J. Chem. Phys.* **1988**, *88*, 922.
(32) Gonzalez, C.; Schlegel, H. B. *J. Chem. Phys.* **1989**, *90*, 2154.
(33) Gonzalez, C.; Schlegel, H. B. *J. Chem. Phys.* **1990**, *94*, 5523.
(34) Raghavachari, K.; Trucks, G. W.; Pople, J. A.; Head-Gordon, M. *Chem. Phys. Lett.* **1989**, *157*, 479.
(35) Dunning, T. H. *J. Chem. Phys.* **1989**, *90*, 1007.
(36) Kendall. R. A.; Dunning, T. H.; Harrison, R. J. *J. Chem. Phys.* **1992**, *96*, 6796.
(37) Woon, D. E.; Dunning, T. H. *J. Chem. Phys.* **1993**, *98*, 1358.
(38) Frisch, M. J.; Trucks, G. W.; Schlegel, H. B.; Scuseria, G. E.; Robb, M. A.; Cheeseman, J. R.; Montgomery, J. A., Jr.; Vreven, T.; Kudin, K. N.; Burant, J. C.; Millam, J. M.; Iyengar, S. S.; Tomasi, J.; Barone, V.; Mennucci, B.; Cossi, M.; Scalmani, G.; Rega, N.; Petersson, G. A.; Nakatsuji, H.; Hada, M.; Ehara, M.; Toyota, K.; Fukuda, R.; Hasegawa, J.; Ishida, M.; Nakajima, T.; Honda, Y.; Kitao, O.; Nakai, H.; Klene, M.; Li, X.; Knox, J. E.; Hratchian, H. P.; Cross, J. B.; Adamo, C.; Jaramillo, J.; Gomperts, R.; Stratmann, R. E.; Yazyev, O.; Austin, A. J.; Cammi, R.; Pomelli, C.; Ochterski, J. W.; Ayala, P. Y.; Morokuma, K.; Voth, G. A.; Salvador, P.; Dannenberg, J. J.; Zakrzewski, V. G.; Dapprich, S.; Daniels, A. D.; Strain, M. C.; Farkas, O.; Malick, D. K.; Rabuck, A. D.; Raghavachari, K.; Foresman, J. B.; Ortiz, J. V.; Cui, Q.; Baboul, A. G.; Clifford, S.; Cioslowski, J.; Stefanov, B. B.; Liu, G.; Liashenko, A.; Piskorz, P.; Komaromi, I.; Martin, R. L.; Fox, D. J.; Keith, T.; Al-Laham, M. A.; Peng, C. Y.; Nanayakkara, A.; Challacombe, M.; Gill, P. M. W.; Johnson, B.; Chen, W.; Wong, M. W.; Gonzalez, C.; Pople, J. A. *Gaussian 03*, revision B.05; Gaussian, Inc.: Pittsburgh, PA, 2003.
(39) Gutsev, G. L.; Sobolewski, A. L.; Adamowicz, L. *Chem. Phys.* **1995**, *196*, 1.
(40) Koch, R.; Wiedel, B.; Anders E. *J. Org. Chem.* **1996**, *61* (7), 2523.
(41) Flügge, J.; Takeo, H.; Yliniemelä, A. *J. Mol. Struct.: THEOCHEM* **1997**, *389*, 27.
(42) Salpin, J.-Y.; Nguyen, M. T. *J. Phys. Chem. A* **1999**, *103* (7), 938.
(43) Zhu, H.-S.; Ho, J.-J. *J. Phys. Chem. A* **2001**, *105*, 6543.